Available online at www.sciencedirect.com

ScienceDirect

Catalysis Today 124 (2007) 247–253

CATALYSIS TODAY

www.elsevier.com/locate/cattod

Photocatalytic treatment of wastewater from cottonseed processing: Effect of operating conditions, aerobic biodegradability and ecotoxicity

Christos Fotiadis, Nikolaos P. Xekoukoulotakis *, Dionissios Mantzavinos

Department of Environmental Engineering, Technical University of Crete, Polytechneioupolis, GR 73100 Chania, Greece

Abstract

The heterogeneous and homogeneous UV-A photocatalytic treatment of an acidic waste stream originating from cottonseed processing was investigated. Several TiO_2 samples were screened in heterogeneous slurry experiments and a commercially available TiO_2 anatase (Millennium PC 500) was found to be considerably more active than the rest. The effect of key operating conditions such as effluent dilution (COD from 800 to 8000 mg/L), Millennium TiO_2 loading (from 100 to 1500 mg/L), solution pH (from 2.6 to 10) and the water matrix (presence of effluent solids and dissolved oxygen) on treatment efficiency was also studied. In general, degradation decreased with increasing effluent concentration, increasing solution pH from acidic to neutral and alkaline conditions and in the absence of oxygen serving as electron acceptor. Experiments with 500 mg/L TiO_2 for 240 min led to nearly complete mineralization at 800 mg/L initial COD but higher catalyst loadings suppressed degradation. Homogeneous experiments with 100 mg/L Fe^{2+} or Fe^{3+} were also performed leading to about 50% COD reduction; this increased to about 65% when H_2O_2 was added, i.e. simulating a Fenton reaction. The original, un-treated effluent was very toxic to marine bacteria *Vibrio fischeri* and very slowly biodegradable aerobically as assessed by shake-flask tests. Nonetheless, a 10-fold dilution (i.e. 800 mg/L COD) eliminated completely ecotoxicity and improved substantially biodegradation rates. On the other hand, photocatalytically pre-treated samples were less biodegradable than the un-treated one. Deep photocatalytic oxidation resulted in decreased ecotoxicity to *V. fischeri*, while moderate photocatalytic oxidation increased toxicity probably due to the formation of toxic intermediates.

Keywords: Biodegradability; Cottonseed oil; TiO_2 photocatalysis; Photo-Fenton; Toxicity; Wastewater

1. Introduction

Cotton is grown in about 70 countries worldwide but 10 of them share about 85% of the world production, namely China, USA, India, Pakistan, Uzbekistan, Brazil, Turkey, Australia, Greece and Syria [1]. In the European Union (EU), only three member states produce cotton at a commercial level, namely Greece, Spain and Portugal with the former being by far the top producer. Greece produced an estimated of 1.125×10^6 metric tonnes of un-ginned cotton in the 2005/2006 market year, with the respective values for Spain and Portugal being 3.55×10^5 and 440 metric tonnes [2]. The EU cotton production represents about 3% of the world production, while EU exports account for about 4% of world cotton exports [1].

Un-ginned cotton is delivered to the gin plant to separate the lint from the seeds. The latter typically undergo further processing onsite and subject to elision to yield valuable by-products, namely cottonseed oil and cake. The production of cottonseed oil (as will be described in detail in following sections) is accompanied by the generation of a strong, organic-containing effluent.

Effluents originating from agro-industrial activities (e.g. olive oil extraction, edible olives processing, wine distilleries, dairy products manufacturing, slaughterhouse, etc.) and indeed other industrial activities usually contain pollutants that are not amenable to direct biological treatment; in this respect, advanced technologies based on chemical oxidation may be the only viable option for decontaminating a biologically recalcitrant effluent [3]. Such advanced oxidation processes (AOPs) include, amongst others, ozone oxidation, hydrogen peroxide, hydrogen peroxide/ferrous or ferric ion (the so-called Fenton's reagent), UV irradiation, photocatalysis, electrochemical oxidation, as well as various combinations of them [4,5].

---

* Corresponding author. Tel.: +30 28210 37796; fax: +30 28210 37847.
E-mail address: nikos.xekoukoulotaki@enveng.tuc.gr
(N.P. Xekoukoulotakis).

0920-5861/$ – see front matter © 2007 Elsevier B.V. All rights reserved.
doi:10.1016/j.cattod.2007.03.042

Table 1
Properties of the effluent from cottonseed oil production used in this study

Property	Value
Chemical oxygen demand, COD (mg/L)	8000
Total organic carbon, TOC (mg/L)	6100
Total suspended solids (mg/L)	200
Total phenols, TP (mg/L)	40
pH	2.6
Color	Pale yellow
Absorbance at 410 nm, I_{410} (a.u.)	0.07
Absorbance at 254 nm, I_{254} (a.u.)	2.2
Ecotoxicity, EC_{50} (%)	22
Ecotoxicity, EC_{20} (%)	16

Over the past several years, heterogeneous semiconductor photocatalysis using TiO_2 as the photocatalyst has received considerable attention for water and wastewater treatment [6–8]. TiO_2 photocatalysis is an emerging wastewater treatment technology with key advantages including the lack of mass transfer limitations, operation at ambient conditions and the possible use of solar irradiation. The catalyst itself is inexpensive, commercially available in various crystalline forms and particle characteristics, non-toxic and photochemically stable.

In addition to heterogeneous processes, homogeneous photocatalysis based on a combination of ultraviolet irradiation, hydrogen peroxide and Fe(II) or Fe(III) (the so-called photo-Fenton reaction) is a cheap and efficient method for water treatment yielding more hydroxyl radicals compared to the conventional Fenton and UV/H_2O_2 systems [9,10].

The aim of this work was to study the treatment of an effluent generated from cottonseed oil production by means of heterogeneous and homogeneous photocatalysis. Emphasis was given on the effect of key operating parameters such as type and loading of catalyst, effluent concentration, solution pH, air sparging, presence of solids on the reduction of the polluting load as well as on effluent aerobic biodegradability and ecotoxicity. To the best of our knowledge, this is the first report dealing with this kind of effluent.

2. Materials and methods

2.1. Origin of the effluent

The effluent was kindly provided by MARKOU SA, a gin plant located in the region of Sterea, central Greece and used as received. The cottonseed processing through which the effluent was generated is as follows: following cotton ginning, the cottonseed is dried with hot air and subsequently undergoes elision in a series of mills and presses. This results in the generation of cottonseed cake and oil; the latter is filtered to remove any solid residues and then neutralized with NaOH, rinsed with water and stored. Neutralization also leads to the formation of soap paste which is then treated with H_2SO_4 to yield oleins and a waste stream; the former are used as fuel in the plant. The final effluent consists of the waste streams from the oil neutralization and paste degradation processes (2:1 volumetric ratio) and is sent to an equalization tank where it was taken from. The effluent, whose main properties are shown in Table 1, is highly acidic with a pale yellow color (consistent with its low absorbance at 410 nm) and a COD content of 8000 mg/L. Its aromatic content, as shown by sample absorbance at 254 nm, is quite high, with only a small fraction being due to phenolic compounds. The effluent has relatively low solids content and is strongly ecotoxic to marine bacteria Vibrio fischeri.

2.2. Catalysts

For heterogeneous photocatalytic experiments, six commercially available samples of titanium dioxide were used as received and screened for their relative catalytic activity. The particulars of each catalyst are shown in Table 2.

In addition to the catalysts shown in Table 2, experiments were conducted with fluorinated samples of Hombikat UV100. Fluorination was performed according to the procedures described in detail elsewhere [11]. Fluorinated Hombikat UV100 was in the anatase crystalline form, it had a specific surface area of 248 m^2/g and an average pore diameter of 67.1 Å [12]. Fluorinated TiO_2 suspensions under UV-A irradiation have been reported to produce free hydroxyl radicals. Furthermore, we prepared a TiO_2 catalyst in the laboratory and compared its activity to that of the rest. Catalyst preparation was done according to the procedure described in detail elsewhere [13]. Synthesized TiO_2 was also in the anatase crystalline form, it had a specific surface area of 73.6 m^2/g and an average pore diameter of 30.4 Å [12].

For homogeneous photocatalytic experiments, $FeSO_4·7H_2O$ and $FeCl_3·6H_2O$ were used as catalysts and provided by Aldrich and Riedel-de Haen, respectively. For photo-Fenton experiments, H_2O_2 in the form of 35% (w/w) solution supplied by Merck was used as the oxidant.

Table 2
TiO_2 catalysts used in this study

Catalyst	Crystalline form	Particle size (nm)	Specific surface area (m^2/g)	Supplier
Degussa P-25	80:20 anatase:rutile	20	50	Degussa
Millennium PC 500	Anatase	5–10	287	Millennium Inorganic Chemicals
Tronox AK1	Anatase	20	90	Kerr McGee Chemicals
Tronox TR	Rutile	300	5.5	Kerr McGee Chemicals
Aldrich	Anatase	nd	nd	Aldrich
Hombikat UV100	Anatase	5	>250	Sachtleben Chemie

nd: not determined.

2.3. Photocatalytic experiments

UV-A irradiation was provided by a 400 W, high-pressure mercury lamp (Osram, HQL, MBF-U). The photon flux of the lamp was determined actinometrically using the potassium ferrioxalate method and it was found 1.12×10^{-5} Einstein/s. Experiments were conducted in an immersion well, batch type, laboratory scale photoreactor, purchased from Ace Glass (Vineland, NJ, USA) which is schematically shown in Fig. 1. It is a three compartment apparatus and consists of an inner, double-walled, borosilicate glass housing the lamp (length: 390 mm, outer diameter: 53 mm) and an external cylindrical reaction vessel (length: 310 mm, internal diameter: 73 mm, volume capacity: 350 mL) joined together with an internally threaded connection with the aid of a nylon bushing connector and an O-ring.

The reaction mixture was placed in the external cylindrical reaction vessel and the inner double-walled borosilicate glass was immersed inside the reaction mixture. The lamp was placed inside the inner borosilicate glass and was effectively cooled by a water circulation stream through the double-walled compartment, acting as a cooling water jacket. During photocatalytic experiments, temperature was maintained constant at 32 ± 2 °C. The external reaction vessel was covered with aluminum foil to reflect irradiation exerting the outer wall of the reaction vessel. This reaction geometry is ideal for full exploitation of UV-A irradiation emitted from the lamp.

In a typical heterogeneous photocatalytic run, the original effluent was diluted 10 times with tap water and then 350 mL were loaded in the reaction vessel. The solution was slurried with the appropriate amount of catalyst and magnetically stirred for 30 min in the dark to ensure complete equilibration of adsorption/desorption of organic compounds on the TiO_2 surface. After that period, the UV-A lamp was turned on, while (unless otherwise stated) air was continuously sparged in the liquid and the reaction mixture was continuously stirred. Similar procedures were followed for the homogeneous photocatalytic runs where it was added to the effluent the appropriate amount of iron salt and (if needed) hydrogen peroxide and sparged with air. Most of the runs were carried out at effluent's natural pH (i.e. 2.6); for those runs performed at neutral or alkaline conditions the appropriate volume of 1 M NaOH solution was added. Samples periodically taken from the reactor were centrifuged to remove solid particles and then analyzed for their residual organic concentration, aerobic biodegradability and ecotoxicity.

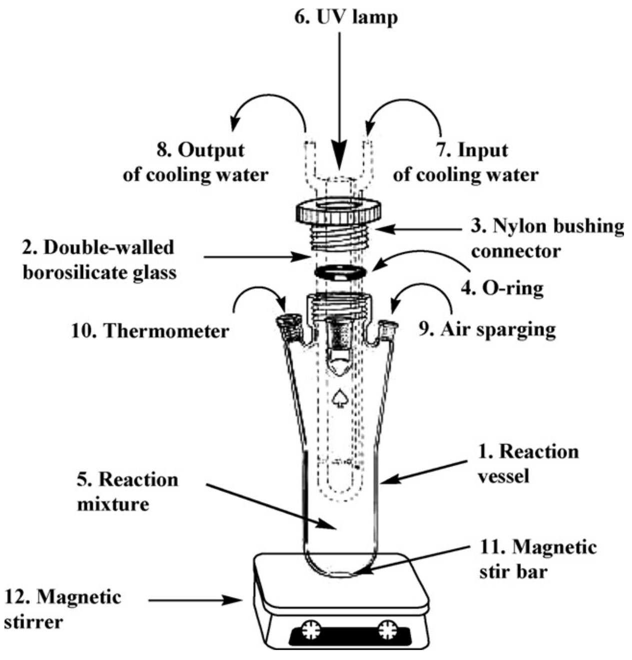

Fig. 1. Schematic representation of the photocatalytic reactor.

2.4. Analytical techniques

COD was determined colorimetrically according to the standard dichromate method, while total phenols according to the Folin-Ciocalteau protocol both of which are described in detail elsewhere [14,15]. Sample absorbance at 254 nm, which is an index of the effluent's aromatic content, was measured on a UV/vis Shimadzu UV 1240 spectrophotometer. TOC was determined colorimetrically at 600 nm with a DR/2010 Hach spectrophotometer using commercially available digestion solutions (Hach Europe, Belgium) for TOC in the range 20–700 mg/L. The appropriate amount of sample was introduced into the digestion solution and the mixture was then incubated for 120 min at 105 °C in a COD reactor (Model 45600-Hach Company, USA).

2.5. Shake-flask tests

Shake-flask experiments were performed to assess the aerobic biodegradability of the effluent prior to and after treatment. Two hundred and fifty-milliliter flasks containing a certain volume of the corresponding effluent and 4 mL of activated sludge taken from the municipal wastewater treatment plant of Chania, Greece were shaken at 150 rpm and 20 °C. Samples periodically drawn from the flasks were filtered with a 0.45 μm disposable filter and analyzed with respect to their COD content as well as biomass growth. The latter was assessed by measuring the absorbance of the sample at 660 nm with a UV/vis Heλios Unicam spectrophotometer.

2.6. Acute ecotoxicity

Acute ecotoxicity to marine bacteria *Vibrio fischeri* was determined measuring inhibition of bioluminescence emitted by the microorganisms before and after their exposure to the effluents in question. The protocol used is described in detail elsewhere [16].

3. Results and discussion

3.1. Heterogeneous photocatalytic degradation

3.1.1. Catalyst screening

Screening runs were conducted to assess the relative catalytic activity of various TiO_2 samples and the results are

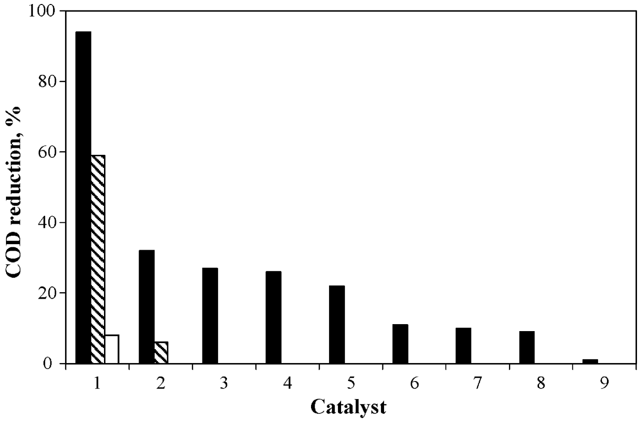

Fig. 2. COD reduction after 240 min of treatment with 500 mg/L of various TiO_2 samples at pH_0 2.6. (1): Millennium PC 500; (2): Tronox AK1; (3): Degussa P-25; (4): Fluorinated Hombikat UV100; (5): TiO_2 prepared in the lab; (6): Tronox TR; (7): no catalyst; (8): Aldrich; (9): Hombikat UV100. Black bar: $COD_0 = 800$ mg/L; hatched bar: $COD_0 = 1600$ mg/L; white bar: $COD_0 = 8000$ mg/L.

shown in Fig. 2. As clearly seen, Millennium PC 500 TiO_2 is highly effective in treating the effluent and leads to nearly complete mineralization after 240 min of reaction. Tronox AK1, Degussa P-25 and the two catalysts that were prepared/modified in the laboratory gave a moderate COD reduction of about 26 ± 4%. For the rest of the catalysts tested, degradation was comparable to that of the respective uncatalyzed run, i.e. at about 10%, except for Hombikat UV100 TiO_2 where COD reduction was almost negligible (about 1%).

To assess catalyst efficiency with respect to the effluent polluting load, experiments were also carried out at increased effluent concentrations, i.e. 1600 mg/L as well as with the original, undiluted effluent and the results are also shown in Fig. 2. Increasing effluent concentration expectedly decreased treatment performance and this was more pronounced for the undiluted effluent with Millennium PC 500 TiO_2. In this respect, all subsequent experiments were performed with Millennium PC 500 TiO_2 samples at an initial effluent concentration of 800 mg/L COD.

The detailed mechanism of the photocatalytic process has been well documented in the literature [4–8] and will be only briefly summarized here. Illumination of an aqueous TiO_2 suspension with irradiation with energy greater than the band gap energy of the semiconductor (i.e. 3.2 eV in the case of anatase TiO_2) generates valence band holes ($h_{\nu h}{}^{+}$) and conduction band electrons ($e_{cb}{}^{-}$). Due to this wide gap energy, anatase can be activated by UV-A irradiation below 385 nm. Holes and electrons may either undesirably recombine liberating heat or make their separate ways to the surface of TiO_2, where they can react with species adsorbed on the catalyst surface. Valence band holes can react with water and hydroxide ions (i.e. under alkaline conditions) to generate hydroxyl radicals $HO^{\bullet}$, while conduction band electrons can react with adsorbed molecular oxygen reducing it to superoxide radical anions which, in turn, reacts with protons to form peroxide radicals:

$$h_{vb}{}^{+} + H_2O \rightarrow HO^{\bullet} + H^{+} \tag{1}$$

$$h_{vb}{}^{+} + OH^{-} \rightarrow HO^{\bullet} \tag{2}$$

$$e_{cb}{}^{-} + O_2 \rightarrow O_2{}^{\bullet -} \tag{3}$$

$$O_2{}^{\bullet -} + H^{+} \rightarrow HO_2{}^{\bullet} \tag{4}$$

The organic compounds present in the wastewater can then undergo both oxidative degradation through their reactions with valence band holes, hydroxyl and peroxide radicals and reductive cleavage through their reaction with electrons yielding various by-products and eventually mineral end products.

3.1.2. Effect of catalyst loading

TiO_2 loading in slurry photocatalytic processes is an important factor that can influence strongly the degradation of organic pollutants. The effect of catalyst loading on conversion was studied in the range 100–1500 mg/L and the extent of COD and TOC reduction after 240 min of reaction is shown in Fig. 3a.

As seen, conversion increases with increasing catalyst loading up to 500 mg/L, while at higher concentrations degradation is adversely affected. The latter is believed to be due to (i) a screening effect of excess catalyst particles, thus masking part of the photosensitive surface and consequently hindering light penetration, and (ii) increased light reflectance onto the catalyst surface both of which occur at increased catalyst concentrations [17]. Interestingly, organic carbon degradation appears to occur predominantly through total

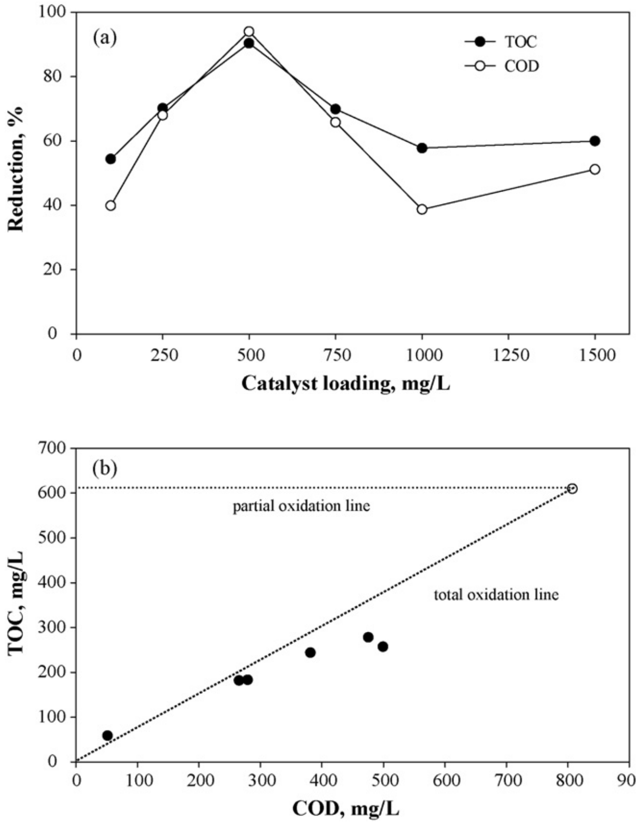

Fig. 3. Effect of Millennium PC 500 TiO_2 loading on treatment efficiency at pH_0 2.6, $COD_0 = 800$ mg/L and 240 min of reaction. (a) TOC and COD reduction at various loadings and (b) relationship between TOC and COD values.

rather than partial oxidation reactions as clearly seen in Fig. 3b where TOC is plotted against COD. The horizontal dotted line corresponds to ideal partial oxidation, i.e. TOC would remain unchanged throughout the reaction and COD would decrease, while the diagonal dotted line corresponds to ideal total oxidation, i.e. COD would decrease linearly with TOC. It is evident that, at the experimental conditions of Fig. 3, total oxidation dominates over partial oxidation during the photocatalytic cottonseed effluent treatment.

3.1.3. *Effect of effluent pH*

To assess the effect of solution pH on effluent treatment, runs were conducted at acidic, near-neutral and alkaline conditions at 250 and 500 mg/L Millennium PC 500 TiO_2 loading and the results are shown in Fig. 4. As seen, degradation is strongly dependent on solution pH and is inhibited at near-neutral or alkaline conditions.

The effect of pH on degradation is a complex issue closely related to the properties of the substrate in question, the amphoteric behavior of TiO_2, as well as the lowering of the oxidative power of the photogenerated holes by increasing the pH value. At pH values greater than about 6.2 (this value corresponds to the point of zero charge for Millennium PC 500 TiO_2 [18]) the catalyst surface becomes negatively charged, thus preventing the hydroxide anion from adsorbing onto the surface, reacting with the holes and consequently yielding hydroxyl radicals. Moreover, the photogenerated electrons are repulsed from the negatively charged surface and, therefore, are not given the chance to react with molecular oxygen to form eventually perhydroxyl radicals; these phenomena would explain to a certain degree the reduced extent of degradation recorded at $pH > 6.2$. The effect of pH on degradation also depends on the effluent properties, i.e. on the assumption that the effluent (whose exact composition is not known) mainly consists of negatively charged species, their adsorption and subsequent photodegradation on the catalyst surface would be favored at acidic rather than neutral/alkaline conditions.

3.1.4. *Effect of solids and aeration*

To examine whether the presence of solids affects the efficiency of photocatalytic treatment, an experiment was conducted with the effluent being filtered first to remove any particles and the results are shown in Fig. 5 alongside the respective run with the unfiltered effluent. Removing the solid content has practically inconsiderable impact on the COD and aromatic contents of the effluent. Interestingly, the aromatic content expressed by sample absorbance at 254 nm appears to increase over the first 15–30 min of reaction and then consistently decreases; this implies that the photocatalytic oxidation of the effluent's organic content yields some aromatic by-products that are oxidized further, thus reducing COD. As can be also seen from Figs. 4 and 5, COD decreases almost linearly with time and this is consistent with a zero order reaction rate.

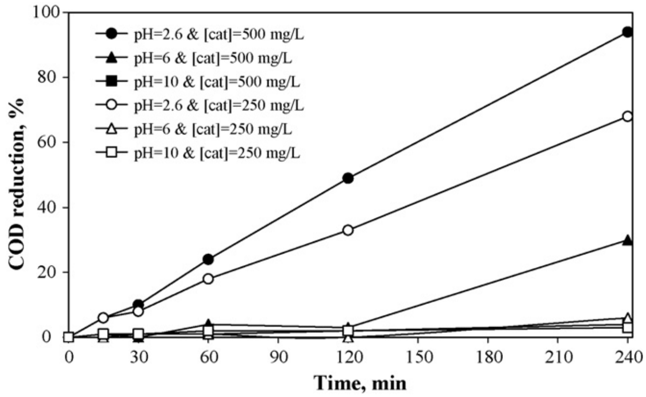

Fig. 4. Effect of starting solution pH on treatment efficiency at COD_0 = 800 mg/L.

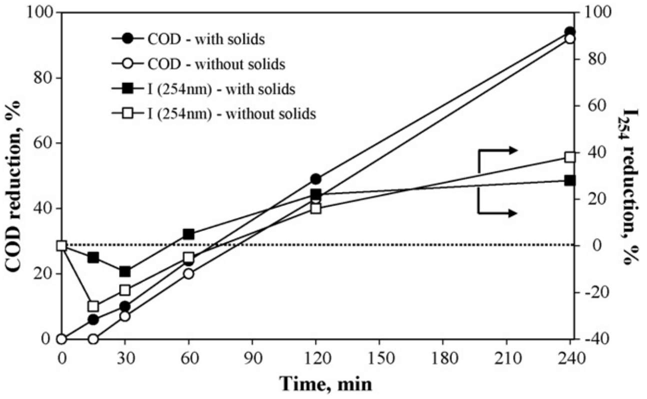

Fig. 5. Temporal change of COD and absorbance at 254 nm during the photocatalytic degradation of filtered and unfiltered effluents at pH_0 2.6 and COD_0 = 800 mg/L.

All runs described so far were performed under air sparging given that the presence of oxygen enhances degradation since it reacts with conduction band electrons (avoiding electron-hole recombination, a major cause of low TiO_2 photocatalytic quantum yield) to form superoxide radical anions that eventually yield reactive hydroxyl radicals. An additional experiment was carried out without air sparging leading to insignificant COD and less than 10% aromatics reduction after 240 min of reaction, thus highlighting the beneficial role of oxygen in the system.

3.2. *Homogeneous photocatalytic degradation*

In recent years, homogeneous photocatalysis using iron as the photocatalyst has received considerable attention for water treatment. This is due to the extremely low cost of the catalyst, the lack of mass transfer limitations that are typically encountered in heterogeneous processes and the potential coupling with hydrogen peroxide to establish the so-called photo-Fenton process as follows:

$$Fe^{2+} + H_2O_2 \rightarrow Fe^{3+} + OH^{\bullet} + OH^{-} \quad (5)$$

$$Fe^{3+} + H_2O + h\nu \rightarrow Fe^{2+} + OH^{\bullet} + H^{+} \quad (6)$$

Reactions (5) and (6) comprise a redox cycle yielding two hydroxyl radicals per molecule of hydrogen peroxide degraded. Fig. 6 shows COD–time profiles during the photocatalytic

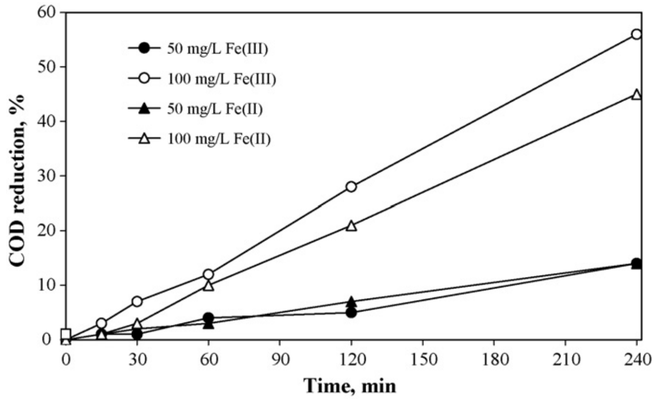

Fig. 6. Temporal change of COD during the photocatalytic degradation with $FeSO_4$ and $FeCl_3$ at pH_0 2.6 and COD_0 = 800 mg/L.

oxidation (without hydrogen peroxide) with ferrous and ferric ions at concentrations of 50 and 100 mg/L.

As seen, 45 and 55% COD reduction could be achieved after 240 min of reaction with 100 mg/L of Fe^{3+} and Fe^{2+}, respectively, and these values decreased to about 15% with decreasing iron concentration to 50 mg/L. Experiments were also performed at 200 mg/L catalyst concentration (data not shown in Fig. 6) and the extent of degradation was similar to that at 100 mg/L. Coupling 100 mg/L Fe^{3+} with 100 mg/L H_2O_2 led to about 65% COD reduction (data also not shown in Fig. 6) and this was followed by about 55% aromatic content reduction; the respective values without hydrogen peroxide were 55 and 26%, thus highlighting the beneficial role of the photo-Fenton process. An additional blank run was performed with 100 mg/L H_2O_2 but without catalyst leading to about 30% COD removal.

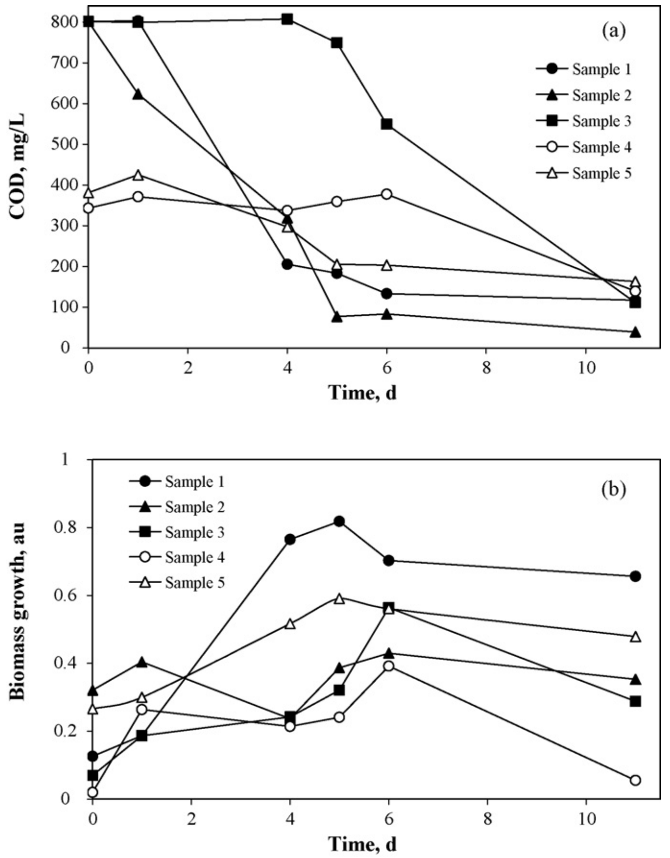

Fig. 7. Evaluation of aerobic biodegradability of diluted (COD_0 = 800 mg/L) cottonseed samples before and after photocatalytic treatment. Sample 1: un-treated at pH_0 2.6; sample 2: un-treated at pH_0 7; sample 3: un-treated at pH_0 2.6 in the presence of 100 mg/L NaN_3; sample 4: pre-treated for 240 min with 100 mg/L Fe^{3+}; sample 5: pre-treated for 240 min with 1500 mg/L Millennium PC 500 TiO_2. (a) COD decrease and (b) biomass change measuring absorbance at 660 nm.

3.3. Effluent biodegradability and ecotoxicity

3.3.1. Aerobic biodegradability

Shake-flask tests with activated sludge taken from the local municipal wastewater treatment plant were performed to assess the aerobic biodegradability of the effluent and the results are shown in Fig. 7. As seen, the diluted, un-treated effluent is slowly biodegradable aerobically even under strongly acidic conditions; following a 24-h lag-phase, biomass grows steeply and this is accompanied by a sharp decrease in COD leading to about 85% removal after 11 days of incubation.

The test was repeated in the presence of 100 mg/L sodium azide, an inhibitor of the biological activity and, in this case, no COD removal was recorded during the first 4–5 days of incubation presumably due to significant bacterial inactivation; this also implies that the reduction of the organic content achieved in the respective run without sodium azide was solely due to biochemical reactions rather than adsorption of organics onto the biomass. However, considerable biomass growth was monitored between days 4 and 6 and this was followed by fast organic degradation leading to 85% COD removal after 11 days. It can be speculated that the amount of NaN_3 used was not enough to destroy completely the microorganisms, part of which managed to recover and grow on the substrate. In addition, NaN_3 might have been decomposed after the first 4–5 days since it is thermo-labile.

Neutral conditions only slightly improved biodegradability leading to about 95% COD removal after 11 days of incubation. An additional test was carried out with the original, un-diluted effluent (data not shown in Fig. 7) at acidic conditions yielding 52% COD degradation after 30 days of incubation.

Two more tests were performed with samples already submitted to homogeneous and heterogeneous photocatalysis during which about 55% COD removal had occurred. In both cases, the rate of biodegradation is clearly lower than that with the un-treated samples comparing the slopes of the respective curves; this may possibly be explained by the fact that (i) the pre-treated samples contain about 50% less metabolic value for the microorganisms, (ii) photocatalytic treatment may have resulted in the formation of less biodegradable by-products, (iii) $FeCl_3$ is partly toxic to biomass and this is consistent with the 6-day lag-phase that occurred during the respective experiment. Nonetheless, the overall COD reduction (i.e. for both photocatalytic and biological oxidation steps) was about 80% at the end of shake-flask tests with both pre-treated samples.

Table 3
Acute ecotoxicity of various samples

Value	Sample 1	Sample 2	Sample 4	Sample 5	Sample 6	Sample 7	Sample 8
EC_{50} (%)	>100	>100	34	42	62	36	>100
EC_{20} (%)	75	93	23	38	40	19	80
Level of toxicity[a]	Non-toxic	Non-toxic	Very toxic	Toxic	Moderately toxic	Very toxic	Non-toxic

Samples 1–5 as in Fig. 7; samples 6–8 as in sample 5 but with 1000, 750 and 500 mg/L TiO_2, respectively.

[a] Based on EC_{50} according to Bennett and Cubbage [19].

3.3.2. Acute ecotoxicity

Although the original, un-diluted effluent is relatively biodegradable aerobically it is still very ecotoxic to *V. fischeri* as seen in Table 1. However, a 10-fold dilution renders the effluent non-toxic as can be seen in Table 3 where toxicity values of various un-treated and pre-treated samples are summarized. As can be seen in Table 3 and Fig. 3a, at moderate photocatalytic oxidation, i.e. when the COD reduction was in the range 40–65% as it was in samples 5, 6 and 7, the photocatalytically pre-treated effluents were more ecotoxic than the un-treated one, thus implying the formation of persistent reaction by-products at considerable concentrations. In the case of homogeneous photocatalysis (sample 4), toxicity may also be attributed to the presence of ferric chloride in the sample. However, treatment with 500 mg/L Millennium PC 500 TiO_2 for 240 min (sample 8) yields a non-toxic effluent presumably due to the fact that deep photocatalytic oxidation had occurred and nearly complete mineralization had achieved (as seen in Fig. 3a).

4. Conclusions

The conclusions drawn from the present study can be summarized as follows:

(1) TiO_2-mediated UV-A photocatalysis is capable of completely degrading an acidic effluent originating from cottonseed oil production which has a strong organic load of several grams per liter COD. Of several commercially available TiO_2 samples tested, anatase Millennium PC 500 was found to be considerably effective in terms of COD and TOC removal.
(2) In heterogeneous photocatalytic treatment, the extent of organic load degradation depends on the operating conditions employed such as the type and concentration of catalyst, initial organic load concentration expressed in terms of COD, solution pH, presence of solids and aeration. At the conditions employed in this study, TiO_2 photocatalytic treatment can result in almost complete mineralization after 240 min of reaction.
(3) Homogeneous photocatalytic treatment using iron as the photocatalyst is less efficient than heterogeneous photocatalysis in degrading the cottonseed wastewater presumably due to the fact that less reactive oxygen species such as hydroxyl radicals are generated photocatalytically. Degradation depends on the initial iron concentration. Coupling of Fe^{3+} with H_2O_2 (i.e. photo-Fenton process) led to increased COD and aromatic content reduction.
(4) The effluent is slowly biodegradable aerobically and highly ecotoxic to marine bacteria *V. fischeri*. A 10-fold dilution is capable of speeding up biodegradation (although several days are still needed to achieve mineralization) as well as eliminating ecotoxicity. Photocatalytically pre-treated samples were more toxic than the un-treated one when the COD and TOC reduction was moderate. On the other hand, when deep photocatalytic oxidation had occurred (i.e. high COD and TOC removal) a decreased ecotoxicity to *V. fisheri* was observed.

Acknowledgments

This work was supported by the Hellenic Ministry of National Education & Religious Affairs under the ‘‘PYTHAGORAS’’ program. The authors wish to thank Dr. M. Ruiz for her assistance with toxicity analysis.

References

[1] United States Department of Agriculture, Foreign Agricultural Service, URL: http://www.fas.usda.gov/psdonline/psdHome.aspx.
[2] Commission regulation (EC) 871/2006, Official Journal of the European Union, L 164/3, June 16, 2006.
[3] D. Mantzavinos, E. Psillakis, J. Chem. Technol. Biotechnol. 79 (2004) 431.
[4] S. Parsons, Advanced Oxidation Processes for Water and Wastewater Treatment, IWA Publishing, Cornwall, UK, 2004.
[5] T. Oppenländer, Photochemical Purification of Water and Air, Wiley–VCH, Weinheim, Germany, 2003.
[6] P.R. Gogate, A.B. Pandit, Adv. Environ. Res. 8 (2004) 501.
[7] D. Mantzavinos, N. Kalogerakis, Environ. Int. 31 (2005) 289.
[8] P.K.J. Robertson, D.W. Bahnemann, J.M.C. Robertson, F. Wood, in: P. Boule, D.W. Bahnemann, P.K.J. Robertson (Eds.), Environmental Photochemistry, Part II, Springer-Verlag, Berlin, 2005 , p. 367 (Chapter 11).
[9] M.Y. Ghaly, G. Härtel, R. Mayer, R. Haseneder, Waste Manage. 21 (2001) 41.
[10] R. Bauer, H. Fallmann, Res. Chem. Intermed. 23 (1997) 341.
[11] N. Watanabe, S. Horikoshi, H. Hidaka, N. Serpone, J. Photochem. Photobiol. A: Chem. 174 (2005) 229.
[12] A.M.T. Silva, E. Nouli, N.P. Xekoukoulotakis, D. Mantzavinos, Appl. Catal. B: Environ. 73 (2007) 11.
[13] G. Li, L. Li, J. Boerio-Goates, B.F. Woodfield, J. Am. Chem. Soc. 127 (2005) 8659.
[14] M. Gotsi, N. Kalogerakis, E. Psillakis, P. Samaras, D. Mantzavinos, Water Res. 39 (2005) 4177.
[15] D. Atanassova, P. Kefalas, E. Psillakis, Environ. Int. 31 (2005) 275.
[16] P.A. Pekakis, N.P. Xekoukoulotakis, D. Mantzavinos, Water Res. 40 (2006) 1276.
[17] J.M. Herrmann, Catal. Today 53 (1999) 115.
[18] D. Gumy, C. Morais, P. Bowen, C. Pulgarin, S. Giraldo, R. Hajdu, J. Kiwi, Appl. Catal. B: Environ. 63 (2006) 76.
[19] J. Bennett, J. Cubbage, Review and evaluation of Microtox® test for freshwater sediments, Environmental Assessment Program Report, USA, 1992.